

# Distributional outcome regression and its application to modelling continuously monitored heart rate and physical activity

Rahul Ghosal<sup>1</sup>, Sujit K. Ghosh<sup>2</sup>, Jennifer A. Schrack<sup>3</sup>, Vadim Zipunnikov<sup>4</sup>

<sup>1</sup> Department of Epidemiology and Biostatistics, University of South Carolina

<sup>2</sup>Department of Statistics, North Carolina State University

<sup>3</sup> Department of Epidemiology, Johns Hopkins Bloomberg School of Public Health

<sup>4</sup> Department of Biostatistics, Johns Hopkins Bloomberg School of Public Health

January 30, 2023

## Abstract

We propose a distributional outcome regression (DOR) with scalar and distributional predictors. Distributional observations are represented via quantile functions and the dependence on predictors is modelled via functional regression coefficients. DOR expands existing literature with three key contributions: handling both scalar and distributional predictors, ensuring jointly monotone regression structure without enforcing monotonicity on individual functional regression coefficients, providing a statistical inference for estimated functional coefficients. Bernstein polynomial bases are employed to construct a jointly monotone regression structure without over-restricting individual functional regression coefficients to be monotone. Asymptotic projection-based joint confidence bands and a statistical test of global significance are developed to quantify uncertainty for estimated functional regression coefficients. Simulation studies illustrate a good performance of DOR model in accurately estimating the distributional effects. The method is applied to continuously monitored heart rate and physical activity data of 890 participants of Baltimore Longitudinal Study of Aging. Daily heart rate reserve, quantified via a subject-specific distribution of minute-level heart rate, is modelled additively as a function of age, gender, and BMI with an adjustment for the daily distribution of minute-level physical activity counts. Findings provide novel scientific insights in epidemiology of heart rate reserve.

*Keywords:* Distributional Data Analysis; Distribution-on-distribution regression; Quantile function-on-scalar Regression; BLSA; Physical Activity; Heart Rate.

# 1 Introduction

Distributional data analysis is an emerging area of research with diverse applications in digital medicine and health (Augustin et al., 2017; Matabuena et al., 2021; Ghosal et al., 2021; Matabuena and Petersen, 2021), radiomics (Yang et al., 2020), neuroimaging (Tang et al., 2020) among many others. With the advent of modern medical devices and wearables, many studies collect subject-specific high frequency or high density observations including heart rate, physical activity (steps, activity counts), continuously monitored blood glucose, functional and structured brain images, and others. The central idea of distributional data analysis is to capture the distributional aspect in this data and model it within regression frameworks. Thus, distributional data analysis inherently deals with data objects which are distributions typically represented via histograms, densities, quantile functions or other distributional representations. Petersen et al. (2021) provide an in-depth overview of recent developments in this area.

Similar to functional regression models, depending on whether the outcome or the predictor is distributional, there are various types of distributional regression models. Petersen and Müller (2016) and Hron et al. (2016) developed functional compositional methods to analyze samples of densities. For scalar outcome and distributional predictors represented via densities, a common idea has been to transform densities by mapping them to a proper Hilbert space  $\mathcal{L}^2$  and then use existing functional regression approaches for modelling scalar outcomes. Petersen and Müller (2016) used a log-quantile density transformation, whereas Talská et al. (2021) used a centered log-ratio transformation. Other approaches for modelling scalar outcomes and distributional predictors include scalar-on-quantile function regression (Ghosal et al., 2021), kernel-based approaches using quantile functions (Matabuena and Petersen, 2021) and many others (see Petersen et al. (2021), Chen et al. (2021) and references therein).

In parallel, there was also a substantial work on developing models with distributional outcome and scalar predictors. Yang et al. (2020) developed a quantile function-on-scalar (QFOSR) regression model, where subject-specific quantile functions of data were modelled via scalar predictors of interest using a function-on-scalar regression approach (Ramsay and Silverman, 2005), which make use of data-driven basis functions called quantlets. One limitation of the approach is a no guarantee of underlying monotonicity of the predicted quantile functions. To address this, Yang (2020) extended this approach

using I-splines (Ramsay et al., 1988) or Beta CDFs which enforce monotonicity at the estimation step. One important limitation of this approach is enforcement of jointly monotone (non-decreasing) regression structure via enforcement of monotonicity on each individual functional regression coefficients. As we demonstrate in our application, this assumption could be too restrictive in real world.

Distribution-on-distribution regression models when both outcome and predictors are distributions have been studied by Verde and Irpino (2010); Irpino and Verde (2013); Chen et al. (2021); Ghodrati and Panaretos (2021); Pegoraro and Beraha (2022). These models aim to understand the association between distributions within a pre-specified, often linear, regression structure. Verde and Irpino (2010); Irpino and Verde (2013) used an ordinary least square approach based on the squared  $\mathcal{L}^2$  Wasserstein distance between distributions. Outcome quantile function  $Q_{iY}(p)$  was modelled as a non-negative linear combination of other quantile functions  $Q_{iX_j}(p)$ s using a multiple linear regression. This model although useful and adequate for some applications, may not be flexible enough as it assumes a linear association between the distribution valued response and predictors, which are additionally assumed to be constant across all quantile levels  $p \in (0, 1)$ . Chen et al. (2021) used a geometric approach taking distributional valued outcome and predictor to a tangent space, where regular tools of function-on-function regression (Ramsay and Silverman, 2005; Yao et al., 2005) were applied. Pegoraro and Beraha (2022) used an approximation of the Wasserstein space using monotone B-spline and developed methods for PCA and regression for distributional data. Recently, Ghodrati and Panaretos (2021) developed a shape-constrained approach linking Frechet mean of the outcome distribution to the predictor distribution via an optimal transport map that was estimated by means of isotonic regression.

Many of above-mentioned methods mainly focused on dealing with constraints enforced by a specific functional representation. Developing inferential tools is somewhat under-developed are of distributional data analysis. Chen et al. (2021) derived the asymptotic convergence rates for the estimated regression operator in their proposed method for Wasserstein regression. Yang et al. (2020) developed joint credible bands for distributional effects, but monotonicity of the quantile function was not imposed. Yang (2020) developed a global statistical test for estimated functional coefficients in the distributional outcome regression, however, no confidence bands was proposed to identify and

test local quantile effects.

In this paper, we propose a distributional outcome regression that expands existing literature in three main directions. First, our model includes both scalar and distributional predictors. Second, it ensures jointly monotone (non-decreasing) additive regression structure without enforcing monotonicity of individual functional regression coefficients. Thirdly, it provides a toolbox of statistical inference tools for estimated functional coefficients including asymptotic projection-based joint confidence bands and a statistical test of global significance. We capture distributional aspect in outcome and predictors via quantile functions and construct a jointly monotone regression model via a specific shape-restricted functional regression model. The distributional effects of the scalar covariates are captured via functional coefficient  $\beta_j(p)$ 's varying over quantile levels and the effect of the distributional predictor is captured via a monotone function  $h(\cdot)$ , similar to an optimal transport approach in [Ghodrati and Panaretos \(2021\)](#). In the special case, when there is no distributional predictor, the model resembles a quantile function-on-scalar regression model, but with much more flexible constraints compared to [Yang \(2020\)](#). In the absence of scalar predictors the model reduces to a distribution on distribution regression model, where the monotone function representing the optimal transport map is estimated by a non-parametric functional regression model under shape constraints. We use Bernstein polynomial (BP) basis functions to model the distributional effects  $\beta_j(p)$ s and the monotone map  $h(\cdot)$ , which are known to enjoy attractive and optimal shape-preserving properties ([Lorentz, 2013](#); [Carnicer and Pena, 1993](#)). Additionally, BP is instrumental in constructing and enforcing a jointly monotone regression structure without over-restricting individual functional regression coefficients to be monotone. Finally, inferential tools are developed including joint asymptotic confidence bands for distributional functional effects and p-values for testing the distributional effects of predictors.

As a motivating application, we study continuously monitored heart rate and physical activity collected in Baltimore Longitudinal Study of Aging (BLSA). We aim to study the association between the distribution of heart rate as a distributional outcome and age, sex and body mass index (BMI) while also adjusting for a key confounder, the distribution of minute-level physical activity aggregated over 8am-8pm time period. Figure 1 displays daily profiles of heart rate and physical activity between 8am-8pm for a BLSA participant

along with the corresponding subject-specific quantile functions.

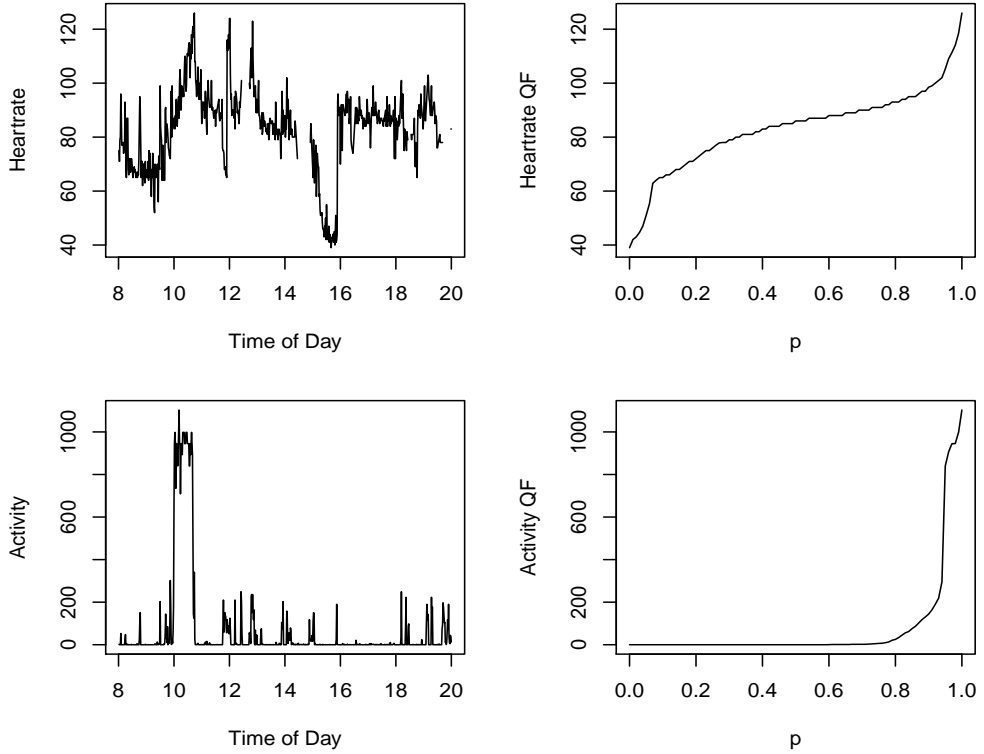


Figure 1: Diurnal profile of heart rate and physical activity between 8 a.m.- 8 p.m. and the corresponding subject specific quantile functions for a randomly chosen subject in the BLSA.

The rest of this article is organized as follows. We present our distributional modeling framework and illustrate the proposed estimation method in Section 2. In Section 3, we perform numerical simulations to evaluate the performance of the proposed method and provide comparisons with existing methods for distributional regression. In Section 4, we demonstrate application of the proposed method in modelling continuously monitored heart rate reserve in BLSA study. Section 5 concludes with a brief discussion of our proposed method and some possible extensions of this work.

## 2 Methodology

### 2.1 Modelling Framework and Distributional Representations

We consider the scenario, where there are repeated subject-specific measurements of a distributional response  $Y$  along with several scalar covariates  $z_j$ ,  $j = 1, 2, \dots, q$  and we

also have a distributional predictor  $X$ . Let us denote the subject-specific response and covariates as  $Y_{ik}, X_{il}, z_{ij}$  ( $k = 1, \dots, n_{1i}, l = 1, \dots, n_{2i}$ ), for subject  $i = 1, \dots, n$ . Here  $n_{1i}, n_{2i}$  denotes the number of repeated observations of the distributional response and predictor respectively for subject  $i$ . Assume  $Y_{ik}$  ( $k = 1, \dots, n_{1i}$ )  $\sim F_{iY}(y)$ , a subject-specific cumulative distribution function (cdf), where  $F_{iY}(y) = P(Y_{ik} \leq y)$ . Then, the subject-specific quantile function is defined as  $Q_{iY}(p) = \inf\{y : F_{iY}(y) \geq p\}, p \in [0, 1]$ . The quantile function completely characterizes the distribution of the individual observations. Given  $Y_{ik}$ 's, the empirical quantile function can be calculated based on linear interpolation of order statistics (Parzen, 2004) and serves as an estimate of the latent subject specific quantile function  $Q_{iY}(p)$  (Yang et al., 2020; Yang, 2020). In particular, for a sample  $(X_1, X_2, \dots, X_n)$ , let  $X_{(1)} \leq X_{(2)} \leq \dots \leq X_{(n)}$  be the corresponding order statistics. The empirical quantile function, for  $p \in [\frac{1}{n+1}, \frac{n}{n+1}]$ , is then given by,

$$\hat{Q}(p) = (1 - w)X_{([(n+1)p])} + wX_{([(n+1)p]+1)}, \quad (1)$$

where and  $w$  is a weight satisfying  $(n+1)p = [(n+1)p] + w$ . Based on this formulation and observations  $Y_{ik}, X_{il}$ , we can obtain the subject specific quantile functions  $\hat{Q}_{iY}(p)$  and  $\hat{Q}_{iX}(p)$  which are estimators of the true quantile functions  $Q_{iY}(p), Q_{iX}(p)$ . The empirical quantile functions are consistent (Parzen, 2004) and are suitable for distributional representaiton for several attractive mathematical properties (Powley, 2013; Ghosal et al., 2021) without requiring any smoothing parameter selection as in density estimation.

## 2.2 Distribution-on-scalar and Distribution Regression

We assume that the scalar covariates  $(z_1, z_2, \dots, z_q) \in [0, 1]^q$  without any loss of generality (e.g., achievable by linear transformation). We posit the following distributional regression model, associating the distributional response  $Q_{iY}(p)$  to the scalar covariates  $z_{ij}$ ,  $j = 1, 2, \dots, q$ , and a distributional predictor  $Q_{iX}(p)$ . We will refer to this as a distribution-on-scalar and distribution regression (DOSDR) model.

$$Q_{iY}(p) = \beta_0(p) + \sum_{j=1}^q z_{ij}\beta_j(p) + h(Q_{iX}(p)) + \epsilon_i(p). \quad (2)$$

Here  $\beta_0(p)$  is a distributional intercept and  $\beta_j(p)$  s are the distributional effects of the scalar covariates  $Z_j$  at quantile level  $p$ . The unknown nonparametric function  $h(\cdot)$  captures the additive effect of the distributional predictor  $Q_{iX}(p)$ . The residual error process  $\epsilon_i(p)$  is assumed to be a mean zero stochastic process with an unknown covariance structure. We make the following flexible and interpretable assumptions on the coefficient functions  $\beta_j(\cdot)$ ,  $j = 0, 1, \dots, q$  and on  $h(\cdot)$  which ensures the predicted value of the response quantile function  $Q_{iY}(p)$  conditionally on the predictors,  $E(Q_{iY}(p) | z_{i1}, z_{i2}, \dots, z_{iq}, q_{ix}(p))$  is non-decreasing.

**Theorem 1** *Let the following conditions hold in the model (2).*

1. *The distributional intercept  $\beta_0(p)$  is non-decreasing.*
2. *Any additive combination of  $\beta_0(p)$  with distributional slopes  $\beta_j(p)$  is non-decreasing, i.e.,  $\beta_0(p) + \sum_{k=1}^r \beta_{j_k}(p)$  is non-decreasing for any sub-sample  $\{j_1, j_2, \dots, j_r\} \subset \{1, 2, \dots, q\}$ .*
3.  *$h(\cdot)$  is non-decreasing.*

*Then  $E(Q_Y(p) | z_1, z_2, \dots, z_q, q_x(p))$  is non-decreasing.*

Note that  $E(Q_Y(p) | z_1, z_2, \dots, z_q, q_x(p))$  is the predicted quantile function under the squared Wasserstein loss function, which is same as the squared error loss for the quantile functions. The proof is illustrated in Appendix A of the Supplementary Material. Assumptions (1) and (2) are much weaker and flexible than the monotonicity conditions of the QFOSR model in [Yang \(2020\)](#), where each of the function coefficients  $\beta_j(p)$ s is required to be monotone, whereas, we only impose monotonicity on the sum of functional coefficients. This is not just a technical aspect but this flexibility is important from a practical perspective, as it allows for capturing possible non-monotone association between the distributional response and individual scalar predictors  $z_j$ 's while still maintaining the required monotonicity of the predicted response quantile function. Condition (3) matches with the monotonicity assumption of the distributional regression model in [Ghodrati and Panaretos \(2021\)](#) and in the absence of any scalar predictors, essentially captures the optimal transport map between the two distributions. Note that this optimal transport map is constructed after adjusting for scalars of interest - thus, it provides a model general inferential framework compared to that in [Ghodrati and Panaretos \(2021\)](#). Thus, the above

DOSDR model extends the previous inferential framework for distributional response on scalar and contains both the QFOSR model and the distribution-on-distribution regression model as its submodels. More succinctly, in absence of distributional predictor we have,

$$Q_{iY}(p) = \beta_0(p) + \sum_{j=1}^q z_{ij} \beta_j(p) + \epsilon_i(p), \quad (3)$$

which is a quantile-function-on-scalar regression (QFOSR) model ensuring monotonicity under conditions (1),(2). Similarly, in absence of any scalar covariates, we have a distribution-on-distribution regression model

$$Q_{iY}(p) = \beta_0(p) + h(Q_{iX}(p)) + \epsilon_i(p). \quad (4)$$

Model (4) is a bit more general than the one considered in [Ghodrati and Panaretos \(2021\)](#), including a transnational effect  $\beta_0(p)$ . As a technical note, in models (2) and (4), function  $h(\cdot)$  is identifiable only up to an additive constant, and in particular, the estimable quantity is the additive effect  $\beta_0(p) + h(q_x(p))$  for a fixed  $Q_X(p) = q_x(p)$ .

### 2.3 Estimation in DOSDR

We follow a shape constrained estimation approach ([Ghosal et al., 2022a](#)) for estimating the distributional effects  $\beta_j(p)$  and the nonparametric function  $h()$  which naturally incorporates the constraints (1)-(3) of Theorem 1 in the estimation step. The univariate coefficient functions  $\beta_j(p)$  ( $j = 0, 1, \dots, p$ ) are modelled in terms of univariate expansions of Bernstein basis polynomials as

$$\beta_j(p) = \sum_{k=0}^N \beta_{jk} b_k(p, N), \quad \text{where } b_k(p, N) = \binom{N}{k} p^k (1-p)^{N-k}, \quad \text{for } 0 \leq p \leq 1. \quad (5)$$

The number of basis polynomials depends on the degree of the polynomial basis  $N$  (which is assumed to be same for all  $\beta_j(\cdot)$  for computational tractability in this paper). The Bernstein polynomials  $b_k(p, N) \geq 0$  and  $\sum_{k=0}^N b_k(p, N) = 1$ . [Wang and Ghosh \(2012\)](#) and [Ghosal et al. \(2022a\)](#) illustrate that various shape constraints e.g., monotonicity, convexity, etc. can be reduced to linear constraints on the basis coefficients of the form  $\mathbb{A}_N \beta_j^N \geq \mathbf{0}$ , where  $\beta_j^N = (\beta_{j0}, \beta_{j1}, \dots, \beta_{jN})^T$  and  $\mathbb{A}_N$  is the constraint matrix chosen in

a way to guarantee a desired shape restriction. In particular, in our context of DOSDR, we need to choose constraint matrices  $\mathbb{A}_N$  in such a way which jointly ensure conditions (1),(2) in Theorem 1 and thus guarantee a non-decreasing predicted value of the response quantile function. The nonparametric function  $h(\cdot)$  is modelled similarly using univariate Bernstein polynomial expansion as

$$h(x) = \sum_{k=0}^N \theta_k b_k(x, N), \text{ where } b_k(x, N) = \binom{N}{k} x^k (1-x)^{N-k}, \text{ for } 0 \leq x \leq 1. \quad (6)$$

Since the domain of  $h(\cdot)$  modelled via Bernstein basis is  $[0, 1]$ , the quantile functions of the distributional predictor  $Q_X(p)$  are transformed to a  $[0, 1]$  scale using linear transformation of the observed predictors. We make the assumption here that the distributional predictors are bounded, which is reasonable in the applications we are interested in. Henceforth, we assume  $Q_X(p) \in [0, 1]$  without loss of generality. Further, note that,  $b_0(x, N) = 1$ , and since  $\beta_0(p)$  already contains this constant term in the DOSDR model (2), including the constant basis while modelling  $h(\cdot)$  will lead to model singularity. Hence we drop the constant basis (i.e. the first term) while modelling  $h(\cdot)$ . In particular,  $h(Q_{iX}(p))$  is modelled as  $h(Q_{iX}(p)) = \sum_{k=1}^N \theta_k b_k(Q_{iX}(p), N)$ . Note that this is equivalent to imposing the constraint  $h(0) = \theta_0 = 0$ . The non-decreasing condition in (3) of Theorem 1 can again be specified as a linear constraint on the basis coefficients of the form  $\mathbb{R}\boldsymbol{\theta} \geq \mathbf{0}$ , where  $\boldsymbol{\theta} = (\theta_1, \dots, \theta_N)^T$ , and  $\mathbb{R}$  is the constraint matrix. The DOSDR model (2) can be reformulated in terms of basis expansions as

$$\begin{aligned} Q_{iY}(p) &= \sum_{k=0}^N \beta_{0k} b_k(p, N) + \sum_{j=1}^q z_{ij} \sum_{k=0}^N \beta_{jk} b_k(p, N) + \sum_{k=1}^N \theta_k b_k(Q_{iX}(p), N) + \epsilon_i(p). \quad (7) \\ &= \mathbf{b}_N(p)^T \boldsymbol{\beta}_0 + \sum_{j=1}^q \mathbf{Z}_{ij}^T(p) \boldsymbol{\beta}_j + \mathbf{b}_N(Q_{iX}(p))^T \boldsymbol{\theta} + \epsilon_i(p). \end{aligned}$$

Here  $\boldsymbol{\beta}_j = (\beta_{j0}, \beta_{j1}, \dots, \beta_{jN})^T$ ,  $\mathbf{b}_N(p)^T = (b_0(p, N), b_1(p, N), \dots, b_N(p, N))$ ,  $\mathbf{b}_N(Q_{iX}(p))^T = (b_1(Q_{iX}(p), N),$

$b_2(Q_{iX}(p), N), \dots, b_N(Q_{iX}(p), N))$  and  $\mathbf{Z}_{ij}^T(p) = z_{ij} * \mathbf{b}_N(p)^T$ . Suppose that we have the quantile functions  $Q_{iY}(p), Q_{iX}(p)$  evaluated on a grid  $\mathcal{P} = \{p_1, p_2, \dots, p_m\} \subset [0, 1]$ . Denote the stacked value of the quantiles for  $i$ th subject as  $\mathbf{Q}_{iY} = (Q_{iY}(p_1), Q_{iY}(p_2), \dots, Q_{iY}(p_m))^T$ .

The DOSDR model in terms of Bernstein basis expansion (7) can be reformulated as

$$\mathbf{Q}_{iY} = \mathbb{B}_0 \boldsymbol{\beta}_0 + \sum_{j=1}^q \mathbb{W}_{ij} \boldsymbol{\beta}_j + \mathbb{S}_i \boldsymbol{\theta} + \boldsymbol{\epsilon}_i, \quad (8)$$

where  $\mathbb{B}_0 = (\mathbf{b}_N(p_1), \mathbf{b}_N(p_2), \dots, \mathbf{b}_N(p_m))^T$ ,  $\mathbb{W}_{ij} = (\mathbf{Z}_{ij}(p_1), \mathbf{Z}_{ij}(p_2), \dots, \mathbf{Z}_{ij}(p_m))^T$  and  $\mathbb{S}_i = (\mathbf{b}_N(Q_{iX}(p_1)),$

$\mathbf{b}_N(Q_{iX}(p_2)), \dots, \mathbf{b}_N(Q_{iX}(p_m)))^T$  and  $\boldsymbol{\epsilon}_i$  are the stacked residuals  $\epsilon_i(p)$ s. The parameters in the above model are the basis coefficients  $\boldsymbol{\psi} = (\boldsymbol{\beta}_0^T, \boldsymbol{\beta}_1^T, \dots, \boldsymbol{\beta}_q^T, \boldsymbol{\theta}^T)^T$ . For estimation of the parameters, we use the following least square criterion, which reduces to a shape constrained optimization problem. Namely, we obtain the estimates  $\hat{\boldsymbol{\psi}}$  by minimizing residual sum of squares as

$$\hat{\boldsymbol{\psi}} = \underset{\boldsymbol{\psi}}{\operatorname{argmin}} \sum_{i=1}^n \|\mathbf{Q}_{iY} - \mathbb{B}_0 \boldsymbol{\beta}_0 - \sum_{j=1}^q \mathbb{W}_{ij} \boldsymbol{\beta}_j - \mathbb{S}_i \boldsymbol{\theta}\|_2^2 \quad s.t \quad \mathbb{D}\boldsymbol{\psi} \geq \mathbf{0}. \quad (9)$$

The universal constraint matrix  $\mathbb{D}$  on the basis coefficients is chosen to ensure the conditions (1),(2),(3) in Theorem 1. Later in this section, we illustrate examples how the constraint matrix is formed in practice. The above optimization problem (9) can be identified as a quadratic programming problem (Goldfarb and Idnani, 1982, 1983). R package `restruktur` (Vanbrabant and Rosseel, 2019) can be used for performing the above optimization.

### Example 1: Single scalar covariate ( $q = 1$ ) and a distributional predictor

We consider the case where there is a single scalar covariate  $z_1$  ( $q = 1$ ) and a distribution predictor  $Q_X(p)$ . In this case, the DOSDR model (2) is given by  $Q_{iY}(p) = \beta_0(p) + z_{i1}\beta_1(p) + h(Q_{iX}(p)) + \epsilon_i(p)$ . The sufficient conditions (1)-(3) for non-decreasing quantile functions in this case reduces to: A) The distributional intercept  $\beta_0(p)$  is non-decreasing B)  $\beta_0(p) + \beta_1(p)$  is non-decreasing C)  $h(\cdot)$  is non-decreasing. Note that the above conditions do not enforce  $\beta_1(p)$  to be non-decreasing. Once the coefficient functions are modelled in terms of Bernstein basis expansions as in (4) and (5), conditions (A)-(C) can be enforced via the following linear restrictions on the basis coefficients i.e.,  $\mathbb{A}_N \boldsymbol{\beta}_0 \geq \mathbf{0}$ ,  $[\mathbb{A}_N \ \mathbb{A}_N](\boldsymbol{\beta}_0^T, \boldsymbol{\beta}_1^T)^T \geq \mathbf{0}$ ,  $\mathbb{A}_{N-1} \boldsymbol{\theta} \geq \mathbf{0}$ . Here  $A_N$  is a constraint matrix which imposes monotonicity on functions  $f_N(x)$  modelled with Bernstein polynomials as  $f_N(x) = \sum_{k=0}^N \beta_k b_k(x, N)$ , where  $b_k(x, N) = \binom{N}{k} x^k (1-x)^{N-k}$ , for  $0 \leq x \leq 1$ . The

derivative is given by  $f'_N(x) = N \sum_{k=0}^{N-1} (\beta_{k+1} - \beta_k) b_k(x, N-1)$ . Hence if  $\beta_{k+1} \geq \beta_k$  for  $k = 0, 1, \dots, N-1$ ,  $f_N(x)$  is non decreasing, which is achieved with the constraint matrix  $\mathbb{A}_N$ . The combined linear restrictions on the parameter  $\psi = (\beta_0^T, \beta_1^T, \theta^T)^T$  is given by  $\mathbb{D}\psi \geq 0$ . The matrices  $\mathbb{A}_N, \mathbb{D}$  are given by

$$\mathbb{A}_N \equiv \begin{pmatrix} -1 & 1 & 0 & \dots & 0 \\ 0 & -1 & 1 & 0 & \dots \\ & & \ddots & & \\ 0 & \dots & 0 & -1 & 1 \end{pmatrix}, \mathbb{D} = \begin{pmatrix} A_N & 0 & 0 \\ A_N & A_N & 0 \\ 0 & 0 & A_{N-1} \end{pmatrix}. \quad (10)$$

Similar example with two scalar covariates ( $q = 2$ ) and a distributional predictor is given in Appendix B of the Supplementary Material. Our estimation ensures that the shape restrictions are enforced everywhere and hence the predicted quantile functions are nondecreasing in the whole domain  $p \in [0, 1]$  as opposed to fixed quantile levels or design points in [Ghodrati and Panaretos \(2021\)](#). The order of the Bernstein polynomial basis  $N$  controls the smoothness of the coefficient functions  $\beta_j(\cdot)$  and  $h(\cdot)$ . We follow a truncated basis approach ([Ramsay and Silverman, 2005](#); [Fan et al., 2015](#)), by restricting the number of BP basis to ensure the resulting coefficient functions are smooth. The optimal order of the basis functions is chosen via  $V$ -fold cross-validation method ([Wang and Ghosh, 2012](#)) using cross-validated residual sum of squares defined as,  $CVSSE = \sum_{v=1}^V \sum_{i=1}^{n_v} \|\mathbf{Q}_{iY,v} - \hat{\mathbf{Q}}_{iY,v}^{-v}\|_2^2$ . Here  $\hat{\mathbf{Q}}_{iY}^{-v}$  is the fitted quantile values of observation  $i$  within the  $v$  th fold obtained from the constrained optimization criterion (9) and trained on the rest ( $V-1$ ) folds.

## 2.4 Uncertainty Quantification and Joint Confidence Bands

To construct confidence intervals, we use the result that the constrained estimator  $\hat{\psi}$  in (9) is the projection of the corresponding unconstrained estimator ([Ghosal et al., 2022a](#)) onto the restricted space:  $\hat{\psi}_r = \underset{\psi \in \Theta_R}{\operatorname{argmin}} \|\psi - \hat{\psi}_{ur}\|_{\hat{\Omega}}^2$ , for a non-singular matrix  $\hat{\Omega}$ . The restricted parameter space is given by  $\Theta_R = \{\psi \in R^{K_n} : \mathbb{D}\psi \geq \mathbf{0}\}$ . The DOSDR model (8) can be reformulated as  $\mathbf{Q}_{iY} = \mathbb{T}_i \psi + \epsilon_i$ , where  $\mathbb{T}_i = [\mathbb{B}_0 \ \mathbb{W}_{i1} \ \mathbb{W}_{i2}, \dots, \mathbb{W}_{iq} \ \mathbb{S}_i]$ . The

unrestricted and restricted estimators are given by,

$$\begin{aligned}\hat{\psi}_{ur} &= \underset{\psi \in R^{Kn}}{\operatorname{argmin}} \sum_{i=1}^n \|\mathbf{Q}_{iY} - \mathbb{T}_i \psi\|_2^2 \\ \hat{\psi}_r &= \underset{\psi \in \Theta_R}{\operatorname{argmin}} \sum_{i=1}^n \|\mathbf{Q}_{iY} - \mathbb{T}_i \psi\|_2^2\end{aligned}\tag{11}$$

Let us denote  $\mathbf{Q}_Y^T = (\mathbf{Q}_{1Y}, \mathbf{Q}_{2Y}, \dots, \mathbf{Q}_{nY})^T$  and  $\mathbb{T} = [\mathbb{T}_1^T, \mathbb{T}_2^T, \dots, \mathbb{T}_n^T]^T$ . Then we can write,

$$\frac{1}{n} \|\mathbf{Q}_Y - \mathbb{T} \psi\|_2^2 = \frac{1}{n} \|\mathbf{Q}_Y - \mathbb{T} \hat{\psi}_{ur}\|_2^2 + \frac{1}{n} \|\mathbb{T} \hat{\psi}_{ur} - \mathbb{T} \psi\|_2^2.$$

Hence  $\hat{\psi}_r = \underset{\psi \in \Theta_R}{\operatorname{argmin}} \|\psi - \hat{\psi}_{ur}\|_{\hat{\Omega}}^2$ , where  $\hat{\Omega} = \frac{1}{n} \sum_{i=1}^n \mathbb{T}_i^T \mathbb{T}_i$  and  $\Omega = E(\hat{\Omega})$  is non-singular.

Thus, we can use the projection of the large sample distribution of  $\sqrt{n}(\hat{\psi}_{ur} - \psi^0)$  to approximate the distribution of  $\sqrt{n}(\hat{\psi}_r - \psi^0)$ . Now  $\sqrt{n}(\hat{\psi}_{ur} - \psi^0)$  is asymptotically distributed as  $N(0, \Delta)$  under suitable regularity conditions (Huang et al., 2004, 2002) for general choice of basis functions (holds true for finite sample sizes if  $\epsilon(p)$  is Gaussian), where  $\Delta$  can be estimated by a consistent estimator. In particular, we use a sandwich covariance estimator corresponding to model  $\mathbf{Q}_{iY} = \mathbb{T}_i \psi + \epsilon_i$ , for estimating  $\Delta$  following a functional principal component analysis (FPCA) approach (Ghosal and Maity, 2022) for estimation of the covariance matrix of the residuals  $\epsilon_i$  ( $i = 1, \dots, n$ ). Details of this estimation procedure is included in Appendix C of the Supplementary Material.

Let us consider the scenario with a single scalar covariate and distributional predictor for simplicity of illustration. The Bernstein polynomial approximation of  $\beta_1(p)$  be given by  $\beta_{1N}(p) = \sum_{k=0}^N \beta_k b_{1k}(p, N) = \rho_{Kn}(p)' \beta_1$ . Algorithm 1 in Appendix D is used to obtain an asymptotic  $100(1 - \alpha)\%$  joint confidence band for the true coefficient function  $\beta_1^0(p)$ , corresponding to a scalar predictor of interest. Here  $\beta_1^0(p)$  denotes the true distributional coefficient  $\beta_1(p)$ . The algorithm relies on two steps i) Use the asymptotic distribution of  $\sqrt{n}(\hat{\psi}_r - \psi^0)$  to generate samples from the asymptotic distribution of  $\hat{\beta}_{1r}(p)$  (these can be used to get point-wise confidence intervals) ii) Use the generated samples and the supremum test statistic (Meyer et al., 2015; Cui et al., 2022) to obtain joint confidence band for  $\beta_1^0(p)$ . Similar strategy can also be employed for obtaining an asymptotic joint confidence band for the additive effect  $\beta_0(p) + h(q_x(p))$ , for a fixed value of  $Q_X(p) = q_x(p)$ . Based on the joint confidence band, it is possible to directly test for the global distributional effects  $\beta(p)$  (or  $h(x)$ ). The p-value for the test

$H_0 : \beta(p) = 0$  for all  $p \in [0, 1]$  versus  $H_1 : \beta(p) \neq 0$  for at least one  $p \in [0, 1]$ , could be obtained based on the  $100(1 - \alpha)\%$  joint confidence band for  $\beta(p)$ . In particular, following [Sergazinov et al. \(2022\)](#), the p-value for the test can be defined as the smallest level  $\alpha$  for which at least one of the  $100(1 - \alpha)\%$  confidence intervals around  $\beta(p)$  ( $p \in \mathcal{P}$ ) does not contain zero. Alternatively, a nonparametric bootstrap procedure for testing the global effects of scalar and distributional predictors is illustrated in Appendix E of the Supplementary Material which could be useful for finite sample sizes and non Gaussian error process.

### 3 Simulation Studies

In this Section, we investigate the performance of the proposed estimation and testing method for DOSDR via simulations. To this end, we consider the following data generating scenarios.

#### 3.1 Data Generating Scenarios

##### Scenario A1: DOSDR, Both distributional and scalar predictor

We consider the DOSDR model given by,

$$Q_{iY}(p) = \beta_0(p) + z_{i1}\beta_1(p) + h(Q_{iX}(p)) + \epsilon_i(p). \quad (12)$$

The distributional effects are taken to be  $\beta_0(p) = 2 + 3p$ ,  $\beta_1(p) = \sin(\frac{\pi}{2}p)$  and  $h(x) = (\frac{x}{10})^3$ . The scalar predictor  $z_{i1}$  is generated independently from a  $U(0, 1)$  distribution. The distributional predictor  $Q_{iX}(p)$  is generated as  $Q_{iX}(p) = c_i Q_N(p, 10, 1)$ , where  $Q_N(p, 10, 1)$  denotes the  $p$ th quantile of a normal distribution  $N(10, 1)$  and  $c_i \sim U(1, 2)$ . The residual error process  $\epsilon(p)$  is independently sampled from  $N(0, 0.1)$  for each  $p$ . Since we do not directly observe these quantile functions  $Q_{iX}(p), Q_{iY}(p)$  in practice we assume we have the subject-specific observations  $\mathcal{X}_i = \{x_{i1} = Q_{iX}(u_{i1}), x_{i2} = Q_{iX}(u_{i2}), \dots, x_{iL_{i1}} = Q_{iX}(u_{iL_{i1}})\}$  and  $\mathcal{Y}_i = \{y_{i1} = Q_{iY}(v_{i1}), y_{i2} = Q_{iY}(v_{i2}), \dots, y_{iL_{i2}} = Q_{iY}(v_{iL_{i2}})\}$ , where  $u_i, v_j$  are independently generated from  $U(0, 1)$  distribution. For simplicity, we assume that  $L_{i1} = L_{i2} = L$  many subject specific observations are available for both the distributional outcome and the predictor. Based on the observations  $\mathcal{X}_i, \mathcal{Y}_i$  the subject specific quantile

functions  $Q_{iX}(p)$  and  $Q_{iY}(p)$  are estimated based on empirical quantiles as illustrated in equation (1) on a grid of  $p$  values  $\in [0, 1]$ . We consider number of individual measurements  $L = 200, 400$  and training sample size  $n = 200, 300, 400$  for this data generating scenario. The grid  $\mathcal{P} = \{p_1, p_2, \dots, p_m\} \subset [0, 1]$  is taken to be a equi-spaced grid of length  $m = 100$  in  $[0.005, 0.995]$ . A separate sample of size  $n_t = 100$  is used as a test set for each of the above cases.

### Scenario A2: DOSDR, Testing the effect of scalar predictor

We consider the data generating scheme (12) in scenario A1 above and test for the distributional effect of the scalar predictor  $z_1$  using the proposed joint-confidence band based test in section 2. To this end we let  $\beta_1(p) = d \times \sin(\frac{\pi}{2}p)$ , where the parameter  $d$  controls the departure from the null hypothesis  $H_0 : \beta_1(p) = 0$  for all  $p \in [0, 1]$  versus  $H_1 : \beta_1(p) \neq 0$  for some  $p \in [0, 1]$ . The number of subject-specific measurements  $L$  is set to 200 and sample sizes  $n \in \{200, 300, 400\}$  are considered.

### Scenario B: DOSDR, Only distributional predictor

We consider the following distribution on distribution regression model

$$Q_{iY}(p) = h(Q_{iX}(p)) + \epsilon_i(p). \quad (13)$$

The distributional outcome  $Q_{iY}(p)$ , the distributional predictor  $Q_{iX}(p)$  and the error process  $\epsilon_i(p)$  are generated similarly as in Scenario A. The number of subject-specific measurements  $L$  is set to 200 and sample sizes  $n \in \{200, 300, 400\}$  are considered. This scenario is used to compare the performance of the proposed DOSDR method with that of the isotonic regression approach illustrated in [Ghodrati and Panaretos \(2021\)](#).

We consider 100 Monte-Carlo (M.C) replications from simulation scenarios A1 and B to assess the performance of the proposed estimation method. For scenario A2, 200 replicated datasets are used to assess type I error and power of the proposed testing method.

### 3.2 Simulation Results

#### Performance under scenario A1:

We evaluate the performance of our proposed method in terms of integrated mean squared error (MSE), integrated squared Bias (Bias<sup>2</sup>) and integrated variance (Var). For the distributional effect  $\beta_1(p)$ , these are defined as  $MSE = \frac{1}{M} \sum_{j=1}^M \int_0^1 \{\hat{\beta}_1^j(p) - \beta_1(p)\}^2 dp$ ,  $Bias^2 = \int_0^1 \{\hat{\beta}_1(p) - \beta_1(p)\}^2 dp$ ,  $Var = \frac{1}{M} \sum_{j=1}^M \int_0^1 \{\hat{\beta}_1^j(p) - \hat{\beta}_1(p)\}^2 dp$ . Here  $\hat{\beta}_1^j(p)$  is the estimate of  $\beta_1(p)$  from the  $j$ th replicated dataset and  $\hat{\beta}_1(p) = \frac{1}{M} \sum_{j=1}^M \hat{\beta}_1^j(p)$  is the M.C average estimate based on the  $M$  replications. Table 1 reports the squared Bias, Variance and MSE of the estimates of  $\beta_1(p)$  for all cases considered in scenario A1. MSE as well as squared Bias and Variance are found to decrease and be negligible as sample size  $n$  or number of measurements  $L$  increase, illustrating satisfactory accuracy of the proposed estimator.

Table 1: Integrated squared bias, variance and mean square error of estimated  $\beta_1(p)$  over 100 Monte-Carlo replications, Scenario A1.

Sample Size	L=200			L=400		
$\beta_1(p)$	Bias <sup>2</sup>	Var	MSE	Bias <sup>2</sup>	Var	MSE
$n= 200$	0.0001	0.0034	0.0035	$2.8 \times 10^{-5}$	0.0019	0.0019
$n= 300$	$1.9 \times 10^{-5}$	0.0026	0.0026	$1.7 \times 10^{-5}$	0.0016	0.0016
$n= 400$	$2.6 \times 10^{-5}$	0.0018	0.0018	$5.5 \times 10^{-6}$	0.0010	0.0010

Since,  $h(x)$  is not directly estimable in the DOSDR model (12), we consider estimation of the estimable additive effect  $\gamma(p) = \beta_0(p) + h(q_x(p))$  at  $q_x(p) = \frac{1}{n} \sum_{i=1}^n Q_{iX}(p)$ . The performance of the estimates in terms of squared Bias, variance and MSE are reported in Table 2, which again illustrates satisfactory performance of the proposed method in capturing the distributional effect of the distributional predictor  $Q_X(p)$ .

Table 2: Integrated squared bias, variance and mean square error of the estimated additive effect  $\gamma(p) = \beta_0(p) + h(q_x(p))$  at  $q_x(p) = \frac{1}{n} \sum_{i=1}^n Q_{iX}(p)$  over 100 Monte-Carlo replications, Scenario A1.

Sample Size	L=200			L=400		
$\beta_0(p) + h(q_x(p))$	Bias <sup>2</sup>	Var	MSE	Bias <sup>2</sup>	Var	MSE
$n= 200$	$9.9 \times 10^{-5}$	0.023	0.023	$4.6 \times 10^{-5}$	0.023	0.023
$n= 300$	$7.3 \times 10^{-5}$	0.017	0.017	$3.2 \times 10^{-5}$	0.017	0.017
$n= 400$	$5.8 \times 10^{-5}$	0.013	0.013	$4.8 \times 10^{-5}$	0.013	0.013

The estimated M.C mean for the distributional effect  $\beta_1(p)$  and  $\gamma(p)$  along with their

respective 95% point-wise confidence intervals are displayed in Figure 2, for the case  $n = 400, L = 400$ . The M.C mean estimates are superimposed on the true curves and along with the narrow confidence intervals, they illustrate low variability and high accuracy of the estimates.

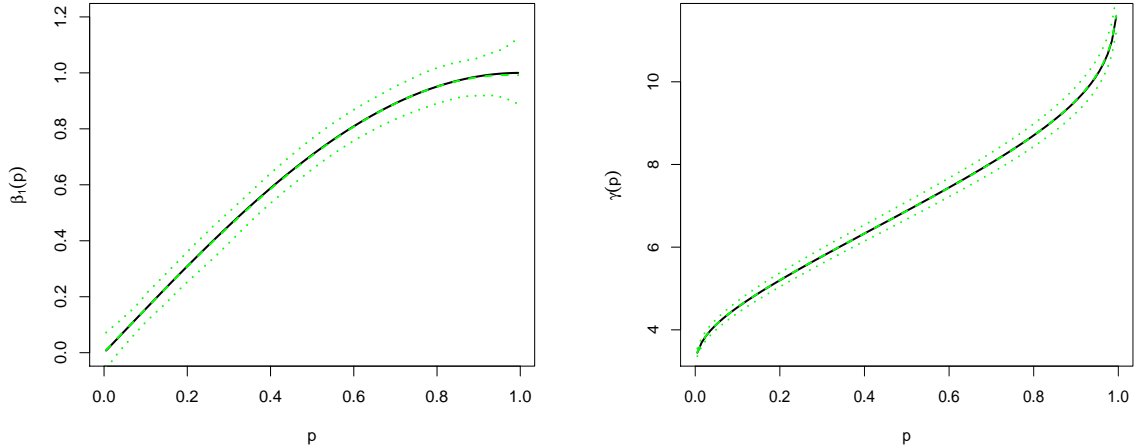


Figure 2: Left: True distributional effect  $\beta_1(p)$  (solid) and estimated  $\hat{\beta}_1(p)$  averaged over 100 M.C replications (dashed) along with point-wise 95% confidence interval (dotted), scenario A1,  $n = 400, L = 400$ . Right: Additive effect  $\gamma(p) = \beta_0(p) + h(q_x(p))$  (solid) at  $q_x(p) = \frac{1}{n} \sum_{i=1}^n Q_{iX}(p)$  and its estimate  $\hat{\gamma}(p)$  averaged over 100 M.C replications (dashed) along with point-wise 95% confidence interval (dotted).

As a measure of out-of-sample prediction performance, we report the average Wasserstein distance between the true quantile functions and the predicted ones in the test set defined as  $WD = \frac{1}{n_t} \sum_{i=1}^{n_t} [\int_0^1 \{Q_i^{test}(p) - \hat{Q}_i^{test}(p)\}^2 dp]^{\frac{1}{2}}$ . Supplementary Table S1 reports the summary of the average Wasserstein distance across the 100 Monte-Carlo replications. The low values of the average  $WD$  metric and their M.C standard error indicate a satisfactory prediction performance of the proposed method. The prediction accuracy appears to be improving with an increase in the number of measurements  $L$ . The performance of the proposed projection based joint confidence intervals for  $\beta_1(p)$  is investigated in Supplementary Table S2 which reports the coverage and width of the joint confidence bands for  $\beta_1(p)$  for various choices of  $N$  and for the case  $L = 200$ . It is observed that the nominal coverage of 95% lies within the two standard error limit of the estimated coverage in the all the cases, particularly for choices of  $N$  picked by our proposed cross

validation method.

## Performance under scenario A2:

We assess the performance of the proposed testing method in terms of estimated type I error and power calculated from the Monte-Carlo replications. We set the order of the Bernstein polynomial basis  $N = 3$  based on our results from previous section. The estimated power curve is displayed as a function of the parameter  $d$  in Supplementary Figure S1, using a nominal level of  $\alpha = 0.05$ . At  $d = 0$ , the null hypothesis holds and the power corresponds to the type I error of the test. The nominal level  $\alpha = 0.05$  lies within its two standard error limit for all the sample sizes, illustrating that the test maintains proper size. For  $d > 0$ , we see the power quickly increase to 1, showing that the proposed test is able to capture small departures from the null hypothesis successfully.

## Performance under scenario B:

We again consider estimation of the estimable additive effect we consider estimation of the estimable additive effect  $\gamma(p) = \beta_0(p) + h(q_x(p))$  at  $q_x(p) = \frac{1}{n} \sum_{i=1}^n Q_{iX}(p)$ , which can be estimated by both the proposed DOSDR (2) method and the isotonic regression method (Ghodrati and Panaretos, 2021). Note that true  $\beta_0(p) = 0$ , but we include a distributional intercept in our DOSDR model, nonetheless, as this information is not available to practitioners. For the isotonic regression method we directly fit the model (13) without any intercept. The performance of the estimates are compared in terms of squared Bias, variance and MSE and are reported in Table 3. We observe a similar performance of the proposed method with the PAVA based isotonic regression method.

Table 3: Integrated squared bias, variance and mean square error of the estimated additive effect  $\gamma(p) = \beta_0(p) + h(q_x(p))$  at  $q_x(p) = \frac{1}{n} \sum_{i=1}^n Q_{iX}(p)$  over 100 Monte-Carlo replications, Scenario B, from the DOSDR method and the isotonic regression method with PAVA (Ghodrati and Panaretos, 2021).

Sample Size	DOSDR			PAVA			
	$\beta_0(p) + h(q_x(p))$	Bias <sup>2</sup>	Var	MSE	Bias <sup>2</sup>	Var	MSE
n= 200	0.0002	0.022	0.022	$2.6 \times 10^{-5}$	0.022	0.022	
n= 300	0.0002	0.016	0.016	$2.4 \times 10^{-5}$	0.016	0.016	
n= 400	0.0002	0.012	0.013	$3 \times 10^{-5}$	0.012	0.012	

The estimated M.C mean for the distributional effect  $\gamma(p)$  along with their respective

95% point-wise confidence intervals are displayed in Supplementary Figure S2, for the case  $n = 400$ . Again, both the method are observed to perform a good job in capturing  $\gamma(p)$ .

The proposed DOSDR method enables conditional estimation of  $\gamma(p) = \beta_0(p) + h(q_x(p))$  on the entire domain  $p \in [0, 1]$ , where as for the isotonic regression method, interpolation is required from grid level estimates. The PAVA based isotonic regression method failed to converge in 5% of the cases for sample size  $n = 200$ , where as, this issue was not faced by our proposed method. In terms of model flexibility, the isotonic regression method do not directly accommodate scalar predictors, or a distributional intercept, and keeping these points in mind our proposed method certainly provide a uniform and flexible approach for modelling distributional outcome, in the presence of both distributional and scalar predictors.

## 4 Modelling Distribution of Heart Rate in Baltimore Longitudinal Study of Aging

In this section, we apply our proposed framework to continuously monitored heart rate and physical activity data collected in Baltimore Longitudinal Study of Aging (BLSA), the longest-running scientific study of aging in the United States. Specifically, the distribution of minute-level heart rate is modelled via age, sex and BMI and the distribution of minute-level activity counts capturing daily composition of physical activity. We set our study period to be 8 a.m. - 8 p.m. and calculate distributional representation of minute-level heart rate and (log-transformed) activity counts of BLSA participants via subject-specific quantile functions  $Q_{iY}(p)$  (heart rate) and  $Q_{iX}(p)$  (represented via log-transformed AC). For each participant, we consider only their first BLSA visit while obtaining the subject-specific quantile functions  $Q_{iY}(p)$ ,  $Q_{iX}(p)$ . Our final sample constitutes of  $n = 890$  BLSA participants, who had heart rate, physical activity and other covariates used for the analysis available. Supplementary Table S3 presents the descriptive statistics of the sample.

Supplementary Figure S3 shows the subject-specific quantile functions of heart rate and physical activity (log-transformed, during 8 a.m.-8 p.m. time period). As a starting point, we study the dependence of mean heart rate on mean activity count and age, sex

(Male=1, Female=0) and BMI via the multiple regression model,

$$\mu_{H,i} = \theta_0 + \theta_1 \text{age}_i + \theta_2 \text{sex}_i + \theta_3 \text{BMI}_i + \theta_4 \mu_{A,i} + \epsilon_i,$$

where  $\mu_{H,i}, \mu_{A,i}$  are the subject specific means of heart rate and activity counts. Supplementary Table S4 reports the results of the model fit. Mean heart rate is found to be negatively associated with age and mean activity, and positively associated with BMI. The above results although useful, does not paint the whole picture about how the distribution of heart rate depends on these biological factors and the distribution of physical activity. Therefore, we use the proposed DOR model

$$Q_{iY}(p) = \beta_0(p) + \text{age}_i \beta_{age}(p) + \text{BMI}_i \beta_{BMI}(p) + \text{sex}_i \beta_{sex}(p) + h(Q_{iX}(p)) + \epsilon_i(p), . \quad (14)$$

The scalar covariates age, BMI as well as activity counts are transformed to be [0, 1] scale using monotone linear transformations. The distributional effects of age, sex (Male=1, Female=0) and BMI on heart rate are captured by  $\beta_{age}(p), \beta_{sex}(p), \beta_{BMI}(p)$ , respectively. The monotone nonparametric function  $h(\cdot)$  is used to link the distribution of heart rate and the distribution of activity counts. We use the proposed estimation method for estimation of the distributional effects  $\beta_j(p)$ s and  $h(\cdot)$  ( $h(0) = 0$  is imposed). The common degree of the Bernstein polynomial basis used to model all the distributional coefficient was chosen via five-fold cross-validation method that resulted in  $N = 5$ . The estimated distributional effects along with their asymptotic 95% joint confidence bands using the proposed projection based method are displayed in Figure 3. The p-values from the joint confidence band based global test for the intercept and the effect of age, BMI, sex, and distribution of activity counts are found to be  $1 \times 10^{-6}, 1 \times 10^{-6}, 5 \times 10^{-5}, 3 \times 10^{-4}$  and  $1 \times 10^{-6}$ , respectively, resulting in the significance of all the predictors.

The estimated distributional intercept  $\hat{\beta}_0(p)$  is monotone and represents the baseline distribution of heart rate. The estimated distributional effect of age is found to be significant for all  $p$ , in particular,  $\hat{\beta}_{age}(p)$  is negative and appears to be decreasing and then stabilizing in  $p \in [0, 1]$  illustrating moderate-high levels of heart rate decrease at an accelerated rate with age compared to sedentary levels of activity (Antelmi et al., 2004). The maximal levels of heart rate ( $p > 0.8$ ) are found to be decreasing with age ( $\beta_{age}(p) < 0$ ) (Kostis et al., 1982; Tanaka et al., 2001; Gellish et al., 2007). The distributional

effect of BMI  $\hat{\beta}_{BMI}(p)$  is found to be positive and increasing in  $p$  (especially at higher quantiles), indicating that a higher maximal heart rate is associated with a higher BMI after adjusting for age, sex and the daily distribution of activity counts (Foy et al., 2018). The estimated effect of sex (Male)  $\hat{\beta}_{sex}(p)$  illustrates that females have higher heart rate (Antelmi et al., 2004; Prabhavathi et al., 2014) compared to males across all quantile levels after adjusting for age, BMI and PA. The lower heart rate in males compared to females can be attributed to size of the heart, which is typically smaller in females than males (Prabhavathi et al., 2014) and thus need to beat faster to provide the same output. The estimated monotone regression map between PA and heart rate distribution  $\hat{h}(x)$  (estimated under constraint  $h(0) = 0$ ) is found to be highly nonlinear and convex, illustrating a non-linear dependence of heart rate on physical activity, especially at higher values of PA. The convex nature of the map points out an accelerated increase in the heart rate quantiles with an increase in the corresponding quantile levels of PA (Leary et al., 2002). The estimated distributional effects especially for age and gender in our analysis, illustrate that the distributional effects have no reason to be non-decreasing, as enforced in the quantile function-on-scalar regression model in Yang (2020), which might lead to wrong conclusions here. The proposed DOR method is more flexible in this regard and enforces the monotonicity of the quantile functions without requiring the distributional effects to be monotone.

We also compare the predictive performance of the proposed DOSDR model with that of the distribution-on-distribution regression model by Ghodrati and Panaretos (2021) based on isotonic regression (DODR-ISO). Supplementary Figure S4 displays the leave-one-out-cross-validated (LOOCV) predicted quantile functions of heart rate from both the methods. We define the measure LOOCV  $R$ -Squared as  $R_{loocv}^2 = 1 - \frac{\sum_{i=1}^N \int_0^1 \{Q_i(p) - \hat{Q}_i^{loocv}(p)\}^2 dp}{\sum_{i=1}^N \int_0^1 \{Q_i(p) - \bar{Q}\}^2 dp}$ , where  $\bar{Q} = \frac{1}{N} \sum_{i=1}^N \int_0^1 Q_i(p) dp$  to compare the out-of-sample prediction accuracy of the two methods. The  $R_{loocv}^2$  value for the DOSDR and the DODR-ISO model are calculated to be 0.60 and 0.49 respectively. This illustrates the proposed DOSDR method is able to predict the heart rate quantile functions more accurately with the use of additional information from the biological scalar factors age, sex and BMI.

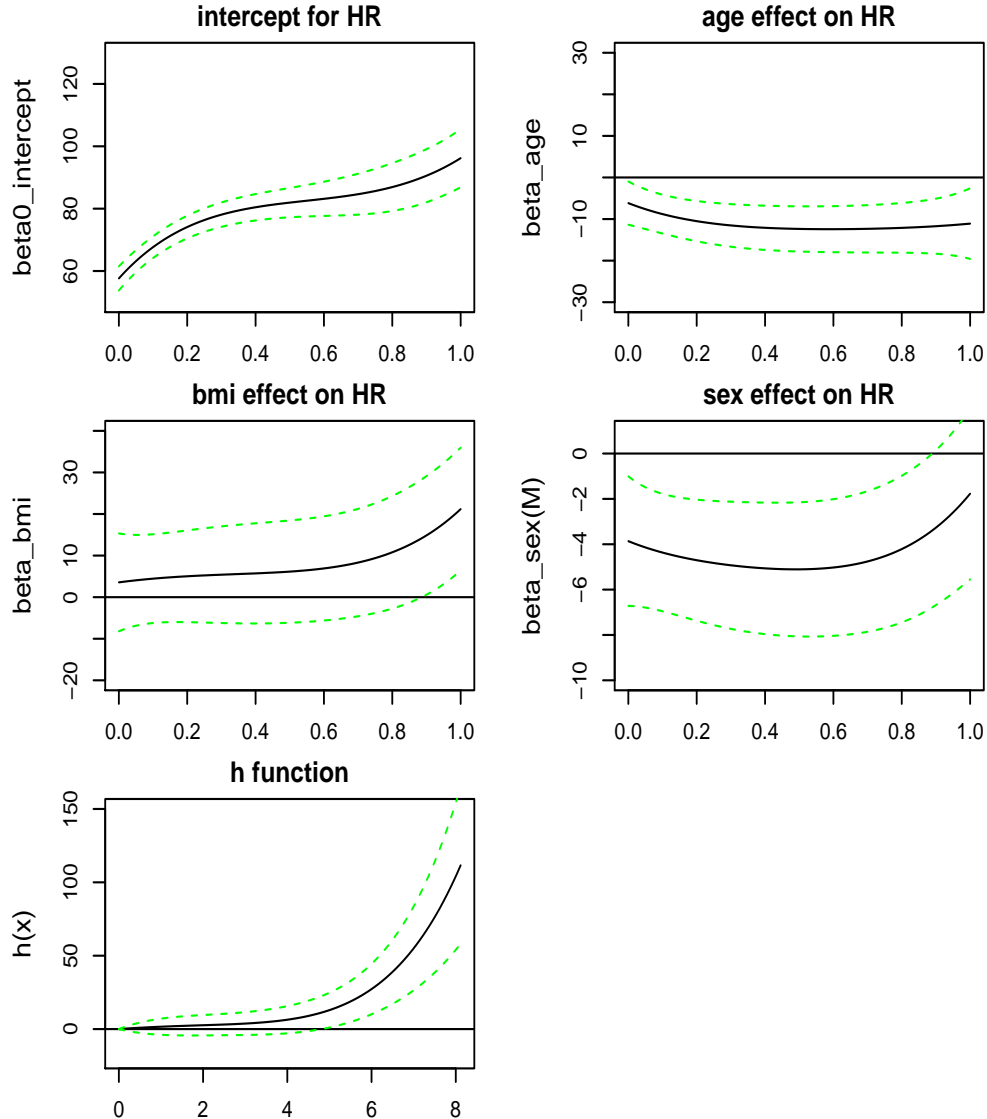


Figure 3: Estimated distributional effects (solid) along with their joint 95% confidence bands (dotted) for age, BMI (both scaled to  $[0, 1]$ ) and sex (Male) on heart rate along with the estimated link function  $h(\cdot)$  (solid) (under the constraint  $h(0) = 0$ ) between the distribution of heart rate and physical activity.

## 5 Discussion

In this article, we have developed a flexible distributional outcome regression. The distributional functional effects are modelled via Bernstein polynomial basis with appropriate shape constraints to ensure monotonicity of the predicted quantile functions. A novel construction of BP-based regression structure results in imposing much less restrictive compared to existing methods for modelling monotone quantile function outcome.

Thus, the proposed framework enables more flexible dependencies between distributional outcome and scalar and distributional predictors. Inferential tools are developed that include projection-based asymptotic joint confidence bands and a global test of statistical significance for estimated functional regression coefficients. Numerical analysis using simulations illustrate an accurate performance of the estimation method. The proposed test is also shown to maintain the nominal test size and have a satisfactory power. An additional nonparametric bootstrap test provided in the supplementary material could be particularly useful in finite sample sizes.

Application of DOR is demonstrated in studying the distributional association between heart rate reserve and key demographics while adjusting for physical activity. Our findings provide important insights about age and gender differences in distribution of heart rate. Beyond the considered epidemiological application, the proposed regression model could be used in other epidemiological studies to more flexibly model distributional aspect of high frequency and high intensity data. Additionally, it can be used for estimation of treatment effects in primary or secondary endpoints quantified via distributions.

There are multiple research directions that remain to be explored based on this current work. In developing our method we have implicitly assumed that there are enough measurements available per subject to accurately estimate quantile functions. Scenarios with only a few sparse measurements pose a practical challenge and will need careful handling. Other aspects of studies collecting distributional data such as distributional measurements being multilevel (Goldsmith et al., 2015) or incorporating spatio-temporal structure (Yang, 2020; Ghosal et al., 2022b) would be important to consider. Another interesting direction of research could be to extend these models beyond the additive paradigm, for example the single index model (Jiang et al., 2011) could be employed to accommodated interaction and nonlinear effects of multiple scalar and distributional predictors. Extending the proposed method to such more general and complex models would be computationally challenging, nonetheless merits future attention because of their potentially diverse applications.

## Supplementary Material

Appendix A-E along with the Supplementary Tables and Supplementary Figures referenced in this article are available online as Supplementary Material.

## Software

Software implementation via R ([R Core Team, 2018](#)) and illustration of the proposed framework is available upon request from the authors.

## References

Antelmi, I., De Paula, R. S., Shinzato, A. R., Peres, C. A., Mansur, A. J., and Grupi, C. J. (2004), “Influence of age, gender, body mass index, and functional capacity on heart rate variability in a cohort of subjects without heart disease,” *The American journal of cardiology*, 93, 381–385.

Augustin, N. H., Mattocks, C., Faraway, J. J., Greven, S., and Ness, A. R. (2017), “Modelling a response as a function of high-frequency count data: The association between physical activity and fat mass,” *Statistical methods in medical research*, 26, 2210–2226.

Carnicer, J. M. and Pena, J. M. (1993), “Shape preserving representations and optimality of the Bernstein basis,” *Advances in Computational Mathematics*, 1, 173–196.

Chen, Y., Lin, Z., and Müller, H.-G. (2021), “Wasserstein regression,” *Journal of the American Statistical Association*, 1–40.

Cui, E., Leroux, A., Smirnova, E., and Crainiceanu, C. M. (2022), “Fast univariate inference for longitudinal functional models,” *Journal of Computational and Graphical Statistics*, 31, 219–230.

Fan, Y., James, G. M., and Radchenko, P. (2015), “Functional additive regression,” *The Annals of Statistics*, 43, 2296–2325.

Foy, A. J., Mandrola, J., Liu, G., and Naccarelli, G. V. (2018), “Relation of obesity to new-onset atrial fibrillation and atrial flutter in adults,” *The American journal of cardiology*, 121, 1072–1075.

Gellish, R. L., Goslin, B. R., Olson, R. E., McDONALD, A., Russi, G. D., and Moudgil, V. K. (2007), “Longitudinal modeling of the relationship between age and maximal heart rate.” *Medicine and science in sports and exercise*, 39, 822–829.

Ghodrati, L. and Panaretos, V. M. (2021), “Distribution-on-Distribution Regression via Optimal Transport Maps,” *arXiv preprint arXiv:2104.09418*.

Ghosal, R., Ghosh, S., Urbanek, J., Schrack, J. A., and Zipunnikov, V. (2022a), “Shape-constrained estimation in functional regression with Bernstein polynomials,” *Computational Statistics & Data Analysis*, 107614.

Ghosal, R. and Maity, A. (2022), “A Score Based Test for Functional Linear Concurrent Regression,” *Econometrics and Statistics*, 21, 114–130.

Ghosal, R., Varma, V. R., Wolfson, D., Hillel, I., Urbanek, J., Hausdorff, J. M., Watts, A., and Zipunnikov, V. (2021), “Distributional data analysis via quantile functions and its application to modelling digital biomarkers of gait in Alzheimer’s Disease,” *Biostatistics*.

Ghosal, R., Varma, V. R., Wolfson, D., Urbanek, J., Hausdorff, J. M., Watts, A., and Zipunnikov, V. (2022b), “Scalar on time-by-distribution regression and its application for modelling associations between daily-living physical activity and cognitive functions in Alzheimer’s Disease,” *Scientific reports*, 12, 1–16.

Goldfarb, D. and Idnani, A. (1982), “Dual and primal-dual methods for solving strictly convex quadratic programs,” in *Numerical analysis*, Springer, pp. 226–239.

— (1983), “A numerically stable dual method for solving strictly convex quadratic programs,” *Mathematical programming*, 27, 1–33.

Goldsmith, J., Zipunnikov, V., and Schrack, J. (2015), “Generalized multilevel function-on-scalar regression and principal component analysis,” *Biometrics*, 71, 344–353.

Hron, K., Menafoglio, A., Templ, M., Hruzova, K., and Filzmoser, P. (2016), “Simplicial principal component analysis for density functions in Bayes spaces,” *Computational Statistics & Data Analysis*, 94, 330–350.

Huang, J. Z., Wu, C. O., and Zhou, L. (2002), “Varying-coefficient models and basis function approximations for the analysis of repeated measurements,” *Biometrika*, 89, 111–128.

— (2004), “Polynomial spline estimation and inference for varying coefficient models with longitudinal data,” *Statistica Sinica*, 14, 763–788.

Irpino, A. and Verde, R. (2013), “A metric based approach for the least square regression of multivariate modal symbolic data,” in *Statistical Models for Data Analysis*, Springer, pp. 161–169.

Jiang, C.-R., Wang, J.-L., et al. (2011), “Functional single index models for longitudinal data,” *The Annals of Statistics*, 39, 362–388.

Kostis, J. B., Moreyra, A., Amendo, M., Di Pietro, J., Cosgrove, N., and Kuo, P. (1982), “The effect of age on heart rate in subjects free of heart disease. Studies by ambulatory electrocardiography and maximal exercise stress test.” *Circulation*, 65, 141–145.

Leary, A. C., Struthers, A. D., Donnan, P. T., MacDonald, T. M., and Murphy, M. B. (2002), “The morning surge in blood pressure and heart rate is dependent on levels of physical activity after waking,” *Journal of hypertension*, 20, 865–870.

Lorentz, G. G. (2013), *Bernstein polynomials*, American Mathematical Soc.

Matabuena, M. and Petersen, A. (2021), “Distributional data analysis with accelerometer data in a NHANES database with nonparametric survey regression models,” *arXiv*.

Matabuena, M., Petersen, A., Vidal, J. C., and Gude, F. (2021), “Glucodensities: a new representation of glucose profiles using distributional data analysis,” *Statistical Methods in Medical Research*, 30, 1445–1464.

Meyer, M. J., Coull, B. A., Versace, F., Cinciripini, P., and Morris, J. S. (2015), “Bayesian function-on-function regression for multilevel functional data,” *Biometrics*, 71, 563–574.

Parzen, E. (2004), “Quantile probability and statistical data modeling,” *Statistical Science*, 19, 652–662.

Pegoraro, M. and Beraha, M. (2022), “Projected Statistical Methods for Distributional Data on the Real Line with the Wasserstein Metric.” *J. Mach. Learn. Res.*, 23, 37–1.

Petersen, A. and Müller, H.-G. (2016), “Functional data analysis for density functions by transformation to a Hilbert space,” *The Annals of Statistics*, 44, 183–218.

Petersen, A., Zhang, C., and Kokoszka, P. (2021), “Modeling Probability Density Functions as Data Objects,” *Econometrics and Statistics*.

Powley, B. W. (2013), “Quantile function methods for decision analysis,” Ph.D. thesis, Stanford University.

Prabhavathi, K., Selvi, K. T., Poornima, K., and Sarvanan, A. (2014), “Role of biological sex in normal cardiac function and in its disease outcome—a review,” *Journal of clinical and diagnostic research: JCDR*, 8, BE01.

R Core Team (2018), *R: A Language and Environment for Statistical Computing*, R Foundation for Statistical Computing, Vienna, Austria.

Ramsay, J. and Silverman, B. (2005), *Functional Data Analysis*, New York: Springer-Verlag.

Ramsay, J. O. et al. (1988), “Monotone regression splines in action,” *Statistical science*, 3, 425–441.

Sergazinov, R., Leroux, A., Cui, E., Crainiceanu, C., Aurora, R. N., Punjabi, N. M., and Gaynanova, I. (2022), “A case study of glucose levels during sleep using fast function on scalar regression inference,” *arXiv preprint arXiv:2205.08439*.

Talská, R., Hron, K., and Grygar, T. M. (2021), “Compositional Scalar-on-Function Regression with Application to Sediment Particle Size Distributions,” *Mathematical Geosciences*, 1–29.

Tanaka, H., Monahan, K. D., and Seals, D. R. (2001), “Age-predicted maximal heart rate revisited,” *Journal of the american college of cardiology*, 37, 153–156.

Tang, B., Zhao, Y., Venkataraman, A., Tsapkini, K., Lindquist, M., Pekar, J. J., and Caffo, B. S. (2020), “Differences in functional connectivity distribution after transcranial direct-current stimulation: a connectivity density point of view,” *bioRxiv*.

Vanbrabant, L. and Rosseel, Y. (2019), *Restricted Statistical Estimation and Inference for Linear Models*, 0.2-250.

Verde, R. and Irpino, A. (2010), “Ordinary least squares for histogram data based on wasserstein distance,” in *Proceedings of COMPSTAT’2010*, Springer, pp. 581–588.

Wang, J. and Ghosh, S. K. (2012), “Shape restricted nonparametric regression with Bernstein polynomials,” *Computational Statistics & Data Analysis*, 56, 2729–2741.

Yang, H. (2020), “Random distributional response model based on spline method,” *Journal of Statistical Planning and Inference*, 207, 27–44.

Yang, H., Baladandayuthapani, V., Rao, A. U., and Morris, J. S. (2020), “Quantile function on scalar regression analysis for distributional data,” *Journal of the American Statistical Association*, 115, 90–106.

Yao, F., Müller, H.-G., and Wang, J.-L. (2005), “Functional linear regression analysis for longitudinal data,” *The Annals of Statistics*, 2873–2903.

# Supplementary Material for Distributional outcome regression and its application to modelling continuously monitored heart rate and physical activity

Rahul Ghosal<sup>1,\*</sup>, Sujit Ghosh<sup>2</sup>, Jennifer A. Schrack<sup>3</sup>, Vadim Zipunnikov<sup>4</sup>

<sup>1</sup> Department of Epidemiology and Biostatistics, University of South Carolina

<sup>2</sup>Department of Statistics, North Carolina State University

<sup>3</sup> Department of Epidemiology, Johns Hopkins Bloomberg School of Public Health

<sup>4</sup> Department of Biostatistics, Johns Hopkins Bloomberg School of Public Health

January 30, 2023

## 1 Appendix A: Proof of Theorem 1

The predicted outcome quantile function is the conditional expectation of the outcome quantile function based on the distribution-on-scalar and distribution regression (DOSDR) model (2) and is given by,

$$E(Q_Y(p) \mid z_1, z_2, \dots, z_q, q_x(p)) = \beta_0(p) + \sum_{j=1}^q z_j \beta_j(p) + h(q_x(p)). \quad (1)$$

We will show conditions (1)-(3) are sufficient conditions to ensure  $E(Q_Y(p) \mid z_1, z_2, \dots, z_q, q_x(p))$  is non-decreasing. Let us assume  $0 \leq z_j \leq 1, \forall j = 1, 2, \dots, J$ , without loss of generality. It is enough to show  $T_1(p) = \beta_0(p) + \sum_{j=1}^q z_j \beta_j(p)$  and  $T_2(p) = h(q_x(p))$  both are non decreasing. The second part is immediate as both  $q_x(\cdot)$  and  $h(\cdot)$  (by condition (3)) are non decreasing. To complete the proof we only need to show  $T_1(p)$  is non decreasing.

$T'_1(p) = \beta'_0(p) + \sum_{j=1}^q z_j \beta'_j(p)$ . Enough to show  $T'_1(p) \geq 0$  for all  $(z_1, z_2, \dots, z_q) \in [0, 1]^q$ . Note that this is a linear function in  $(z_1, z_2, \dots, z_q) \in [0, 1]^q$ . By the well-known Bauer's principle the minimum is attained at the boundary points  $B = \{(z_1, z_2, \dots, z_q) : z_j \in \{0, 1\}\}$ . Hence, the sufficient conditions are  $\beta'_0(p) \geq 0$  and  $\beta'_0(p) + \sum_{k=1}^r \beta'_{j_k}(p) \geq 0$  for any sub-sample  $\{j_1, j_2, \dots, j_r\} \subset \{1, 2, \dots, q\}$ , which follows from condition (1) and (2).

## 2 Appendix B: Example of DOSDR

### Example 2: Two scalar covariates ( $q = 2$ ) and a distributional predictor

We illustrate the estimation for DOSDR where there are two scalar covariates  $z_1, z_2$  ( $q = 1$ ) and a single distribution predictor  $Q_X(p)$ . The DOSDR model (2) is given by  $Q_{iY}(p) = \beta_0(p) + z_{i1} \beta_1(p) + z_{i2} \beta_2(p) + h(Q_{iX}(p)) + \epsilon_i(p)$ . The sufficient conditions (1)-(3) of Theorem 1 in this case reduce to : A) The distributional intercept  $\beta_0(p)$  is non-decreasing. B)  $\beta_0(p) + \beta_1(p)$ ,  $\beta_0(p) + \beta_2(p)$ ,  $\beta_0(p) + \beta_1(p) + \beta_2(p)$  is non-decreasing. C)  $h(\cdot)$  is non-decreasing. Note that condition B) illustrates that as the number of scalar covariates increase we have more and more combinatorial combinations of the coefficient functions restricted to be non-decreasing. Similar to Example 1, Conditions (A)-(C) again become linear restrictions on the basis coefficients of the form  $\mathbb{D}\psi \geq 0$ , where the constraint

matrix is given by  $\mathbb{D} = \begin{pmatrix} A_N & 0 & 0 & 0 \\ A_N & A_N & 0 & 0 \\ A_N & 0 & A_N & 0 \\ A_N & A_N & A_N & 0 \\ 0 & 0 & 0 & A_{N-1} \end{pmatrix}$ .

As the number of restrictions increase the parameter space becomes smaller and smaller, which can result in a faster convergence of the optimization algorithm.

### 3 Appendix C: Estimation of Asymptotic Covariance Matrix

The DOSDR model (8) in the paper was reformulated as

$$\mathbf{Q}_{iY} = \mathbb{T}_i \boldsymbol{\psi} + \boldsymbol{\epsilon}_i,$$

where  $\mathbb{T}_i = [\mathbb{B}_0 \ \mathbb{W}_{i1} \ \mathbb{W}_{i2}, \dots, \mathbb{W}_{iq} \ \mathbb{S}_i]$ . Under suitable regularity conditions (Huang et al., 2004),  $\sqrt{n}(\hat{\boldsymbol{\psi}}_{ur} - \boldsymbol{\psi}^0)$  can be shown to be asymptotically distributed as  $N(0, \Delta)$  (also holds true for finite sample sizes if  $\epsilon(p)$  is Gaussian). In reality,  $\Delta$  is unknown and we want to estimate  $\Delta$  by an estimator  $\hat{\Delta}$ . We derive a sandwich covariance estimator  $\hat{\Delta}$  corresponding to the above model. Based on the ordinary least square optimization criterion for model (11) (of the paper), the unrestricted estimator is given by  $\hat{\boldsymbol{\psi}}_{ur} = (\mathbb{T}^T \mathbb{T})^{-1} \mathbb{T}^T \mathbf{Q}_Y$ , where  $\mathbf{Q}_Y^T = (\mathbf{Q}_{1Y}, \mathbf{Q}_{2Y}, \dots, \mathbf{Q}_{nY})^T$  and  $\mathbb{T} = [\mathbb{T}_1^T, \mathbb{T}_2^T, \dots, \mathbb{T}_n^T]^T$ . Hence,  $Var(\hat{\boldsymbol{\psi}}_{ur}) = (\mathbb{T}^T \mathbb{T})^{-1} \mathbb{T}^T \Sigma \mathbb{T} (\mathbb{T}^T \mathbb{T})^{-1}$ . Here  $\Sigma = Var(\epsilon)$ , which is typically unknown. We apply an FPCA based estimation approach (Ghosal and Maity, 2022) to estimate  $\Sigma$ .

Let us assume (Huang et al., 2004) the error process  $\epsilon(p)$  can be decomposed as  $\epsilon(p) = V(p) + w_p$ , where  $V(p)$  is a smooth mean zero stochastic process with covariance kernel  $G(p_1, p_2)$  and  $w_p$  is a white noise with variance  $\sigma^2$ . The covariance function of the error process is then given by  $\Sigma(p_1, p_2) = cov\{\epsilon(p_1), \epsilon(p_2)\} = G(p_1, p_2) + \sigma^2 I(p_1 = p_2)$ . For data observed on dense and regular grid  $\mathcal{P}$ , the covariance matrix of the residual vector  $\boldsymbol{\epsilon}_i$  is  $\Sigma_{m \times m}$ , the covariance kernel  $\Sigma(p_1, p_2)$  evaluated on the grid  $\mathcal{P} = \{p_1, p_2, \dots, p_m\}$ . We can estimate  $\Sigma(\cdot, \cdot)$  nonparametrically using functional principal component analysis (FPCA) if the original residuals  $\epsilon_{ij}$  were available. Given  $\epsilon_i(p_j)$ s, FPCA (Yao et al., 2005)

can be used to get  $\hat{\phi}_k(\cdot)$ ,  $\hat{\lambda}_k$ s and  $\hat{\sigma}^2$  to form an estimator of  $\Sigma(p_1, p_2)$  as

$$\hat{\Sigma}(p_1, p_2) = \sum_{k=1}^K \hat{\lambda}_k \hat{\phi}_k(p_1) \hat{\phi}_k(p_2) + \hat{\sigma}^2 I(p_1 = p_2),$$

where  $K$  is large enough such that percent of variance explained (PVE) by the selected eigencomponents exceeds some pre-specified value such as 99%.

In practice, we don't have the original residuals  $\epsilon_{ij}$ . Hence we fit the unconstrained DOSDR model (11) and obtain the residuals  $e_{ij} = Q_{iY}(p_j) - \hat{Q}_{iY}(p_j)$ . Then treating  $e_{ij}$  as our original residuals, we can obtain  $\hat{\Sigma}(p_1, p_2)$  and  $\hat{\Sigma}_{m \times m}$  using the FPCA approach outlined above. Then  $\hat{Var}(\epsilon) = \hat{\Sigma} = \text{diag}\{\hat{\Sigma}_{m \times m}, \hat{\Sigma}_{m \times m}, \dots, \hat{\Sigma}_{m \times m}\}$ . [Ghosal and Maity \(2022\)](#) discusses consistency of  $\hat{\Sigma}$  under standard regularity conditions. Hence an consistent estimator of the covariance matrix is given by  $\hat{Var}(\hat{\psi}_{ur}) = (\mathbb{T}^T \mathbb{T})^{-1} \mathbb{T}^T \hat{\Sigma} \mathbb{T} (\mathbb{T}^T \mathbb{T})^{-1}$ . In particular,  $\hat{\Delta}_n = \hat{\Delta}/n = \hat{cov}(\hat{\psi}_{ur}) = (\mathbb{T}^T \mathbb{T})^{-1} \mathbb{T}^T \hat{\Sigma} \mathbb{T} (\mathbb{T}^T \mathbb{T})^{-1}$ .

## 4 Appendix D: Algorithm 1 for Joint Confidence Band

---

**Algorithm 1** Joint confidence band of  $\beta_1^0(p)$

---

1. Fit the unconstrained model and obtain the unconstrained estimator  $\hat{\psi}_{ur} = \underset{\psi \in R^{K_n}}{\operatorname{argmin}} \sum_{i=1}^n \|\mathbf{Q}_{iY} - \mathbb{T}_i \psi\|_2^2$ .
2. Fit the constrained model and obtain the constrained estimator  $\hat{\psi}_r = \underset{\psi \in \Theta_R}{\operatorname{argmin}} \sum_{i=1}^n \|\mathbf{Q}_{iY} - \mathbb{T}_i \psi\|_2^2$ . Obtain the constrained estimator of  $\beta_1^0(p)$  as  $\hat{\beta}_{1r}(p) = \rho_{K_n}(p)' \hat{\beta}_{1r}$ .
3. Let  $\hat{\Delta}_n$  be an estimate of the asymptotic covariance matrix of the unconstrained estimator given by  $\hat{\Delta}_n = \hat{\Delta}/n = \operatorname{cov}(\hat{\psi}_{ur})$
4. For  $b = 1$  to  $B$ 
  - generate  $\mathbf{Z}_b \sim N_{K_n}(\hat{\psi}_{ur}, \hat{\Delta}_n)$ .
  - compute the projection of  $\mathbf{Z}_b$  as  $\hat{\psi}_{r,b} = \underset{\psi \in \Theta_R}{\operatorname{argmin}} \|\psi - \mathbf{Z}_b\|_{\hat{\Omega}}^2$ .
  - End For
5. For each generated sample  $\hat{\psi}_{r,b}$  calculate estimate of  $\beta_1^0(p)$  as  $\hat{\beta}_{1r,b}(p) = \rho_{K_n}(p)' \hat{\beta}_{1r,b}$  ( $b = 1, \dots, B$ ). Compute  $\operatorname{Var}(\hat{\beta}_{1r}(p))$  based on these samples.
6. For  $b = 1$  to  $B$ 
  - calculate  $u_b = \max_{p \in \mathcal{P}} \frac{|\hat{\beta}_{1r,b}(p) - \hat{\beta}_{1r}(p)|}{\sqrt{\operatorname{Var}(\hat{\beta}_{1r}(p))}}$ .
  - End For
7. Calculate  $q_{1-\alpha}$  the  $(1 - \alpha)$  empirical quantile of  $\{u_b\}_{b=1}^B$ .
8.  $100(1 - \alpha)\%$  joint confidence band for  $\beta_1^0(p)$  is given by  $\hat{\beta}_{1r}(p) \pm q_{1-\alpha} \sqrt{\operatorname{Var}(\hat{\beta}_{1r}(p))}$ .

---

## 5 Appendix E: Bootstrap Test for Global Distributional Effects

A practical question of interest in the DOSDR model is to directly test for the global distributional effect of the scalar covariates  $Z_j$  or test for the distributional effect of the distributional predictor  $Q_X(p)$ . In this section, we illustrate an nonparametric bootstrap test based on our proposed estimation method which also easily lends itself to the required

shape constraints of the regression problem. In particular, we obtain the residual sum of squares of the null and the full model and come up with the F-type test statistic defined as

$$T_D = \frac{RSS_N - RSS_F}{RSS_F}. \quad (2)$$

Here  $RSS_N, RSS_F$  are the residual sum of squares under the null and the full model respectively. For example, let us consider the case of testing

$$H_0 : \beta_r(p) = 0 \text{ for all } p \in [0, 1] \quad \text{versus} \quad H_1 : \beta_r(p) \neq 0 \text{ for some } p \in [0, 1].$$

Let  $r = q$  without loss of generality. The residual sum of squares for the full model is given by  $RSS_F = \sum_{i=1}^n \|\mathbf{Q}_{iY} - \mathbb{B}_0 \hat{\boldsymbol{\beta}}_0 - \sum_{j=1}^q \mathbb{W}_{ij} \hat{\boldsymbol{\beta}}_j - \mathbb{S}_i \hat{\boldsymbol{\theta}}\|_2^2$ , where the estimates are obtained from the optimization criterion (9) in the paper, with the constraint  $\mathbb{D}_F \boldsymbol{\psi} \geq \mathbf{0}$  (denoting the constraint matrix for the full model as  $\mathbb{D}_F$ ). Similarly, we have  $RSS_N = \sum_{i=1}^n \|\mathbf{Q}_{iY} - \mathbb{B}_0 \hat{\boldsymbol{\beta}}_0 - \sum_{j=1}^{q-1} \mathbb{W}_{ij} \hat{\boldsymbol{\beta}}_j - \mathbb{S}_i \hat{\boldsymbol{\theta}}\|_2^2$ , where the estimates are again obtained from (9) with the constraint  $\mathbb{D}_N \boldsymbol{\psi} \geq \mathbf{0}$ . Note that, in this case the constraint matrix is denoted by  $D_N$  and this is essentially a submatrix of  $\mathbb{D}_F$  as the conditions for monotinicity in (1)-(3) (Theorem 1) for the reduced model is a subset of the original constraints for the full model. The null distribution of the test statistic  $T_D$  is nonstandard, hence we use residual bootstrap to approximate the null distribution. The complete bootstrap procedure for testing the distributional effect of a scalar predictor is presented in algorithm (2) below. Similar strategy could be employed for testing the distributional effect of a distributional predictor or multiple scalar predictors.

---

**Algorithm 2** Bootstrap algorithm for testing the distributional effect of a scalar predictor

---

1. Fit the full DOSDR model in the paper using the optimization criterion

$$\hat{\psi}_F = \underset{\psi}{\operatorname{argmin}} \sum_{i=1}^n \|\mathbf{Q}_{iY} - \mathbb{B}_0 \boldsymbol{\beta}_0 - \sum_{j=1}^q \mathbb{W}_{ij} \boldsymbol{\beta}_j - \mathbb{S}_i \boldsymbol{\theta}\|_2^2 \quad s.t \quad \mathbb{D}_F \psi \geq \mathbf{0}.$$

and calculate the residuals  $e_i(p_l) = Q_{iY}(p_l) - \hat{Q}_{iY}(p_l)$ , for  $i = 1, 2, \dots, n$  and  $l = 1, 2, \dots, m$ .

2. Fit the reduced model corresponding to  $H_0$  (the null) and estimate the parameters using the minimization criteria,

$$\hat{\psi}_N = \underset{\psi}{\operatorname{argmin}} \sum_{i=1}^n \|\mathbf{Q}_{iY} - \mathbb{B}_0 \boldsymbol{\beta}_0 - \sum_{j=1}^{q-1} \mathbb{W}_{ij} \boldsymbol{\beta}_j - \mathbb{S}_i \boldsymbol{\theta}\|_2^2 \quad s.t \quad \mathbb{D}_N \psi \geq \mathbf{0}.$$

Denote the estimates of the distributional effects as  $\hat{\beta}_j^N(p)$  for  $j = 0, 1, \dots, q-1$  and  $\hat{h}^N(x)$ .

3. Compute test statistic  $T_D$  (2) based on these null and full model fits, denote this as  $T_{obs}$ .
4. Resample  $B$  sets of bootstrap residuals  $\{e_{b,i}^*(p)\}_{i=1}^n$  from residuals  $\{e_i(p)\}_{i=1}^n$  obtained in step 1.
5. for  $b = 1$  to  $B$
6. Generate distributional response under the reduced DOSDR model as

$$Q_{b,iY}^*(p) = \hat{\beta}_0^N(p) + \sum_{j=1}^{q-1} z_{ij} \hat{\beta}_j^N(p) + \hat{h}^N(Q_{iX}(p)) + e_{b,i}^*(p).$$

7. Given the bootstrap data set  $\{Q_{iX}(p), Q_{b,iY}^*(p), z_1, z_2, \dots, z_q\}_{i=1}^n$  fit the null and the full model to compute the test statistic  $T_b^*$ .
8. end for
9. Calculate the p-value of the test as  $\hat{p} = \frac{\sum_{b=1}^B I(T_b^* \geq T_{obs})}{B}$ .

---

## 6 Supplementary Tables

Table S1: Average Wasserstein distance (standard error) between true and predicted quantile functions in the test set over 100 Monte-Carlo replications, Scenario A1.

Sample Size	L=200	L=400
n= 200	0.2587 (0.0154)	0.1882 (0.0138)
n= 300	0.2568 (0.0132)	0.1858 (0.0105)
n= 400	0.2554 (0.0141)	0.1865 (0.0120)

Table S2: Coverage of the projection-based 95% joint confidence interval for  $\beta_1(p)$ , for various choices of the order of the Bernstein polynomial (BP) basis, scenario A1, based on 100 M.C replications with  $L = 200$ . Average width of the joint confidence interval is given in the parenthesis. The average choices of  $N$  from cross-validation for this scenario are highlighted in bold.

BP order (N)	Sample size (n=200)	Sample size (n=300)	Sample size (n=400)
2	0.92 (0.29)	0.9 (0.24)	0.9 (0.20)
3	<b>0.92 (0.31)</b>	0.94 (0.25)	0.96 (0.22)
4	0.93 (0.33)	<b>0.93 (0.26)</b>	<b>0.93 (0.23)</b>

Table S3: Descriptive statistics of age and BMI for the complete, male and female samples in the BLSA analysis.

Characteristic	Complete (n=890)		Male (n=432)		Female (n=458)		P value
	Mean	SD	Mean	SD	Mean	SD	
Age	66.66	13.35	68.03	13.41	65.37	13.17	0.003
BMI (kg/m <sup>2</sup> )	27.40	4.96	27.52	4.23	27.28	5.57	0.45

Table S4: Results from multiple linear regression model of mean heart rate on age, sex (Male), BMI and mean activity count. Reported are the estimated fixed effects along with their standard error and P-values.

Dependent variable : Mean heart rate			
	Value	Std.Error	P-value
Intercept	82.47	3.458	$< 2 \times 10^{-16}***$
age	-0.18	0.026	$< 1.2 \times 10^{-11}***$
sex	-4.19	0.659	$< 3.2 \times 10^{-10}***$
BMI	0.18	0.067	0.0091**
Mean activity	2.44	0.697	0.0005***
Observations	890		
Adjusted R <sup>2</sup>	0.142		

Note:

\*p<0.05; \*\*p<0.01; \*\*\*p<0.001

## 7 Supplementary Figures

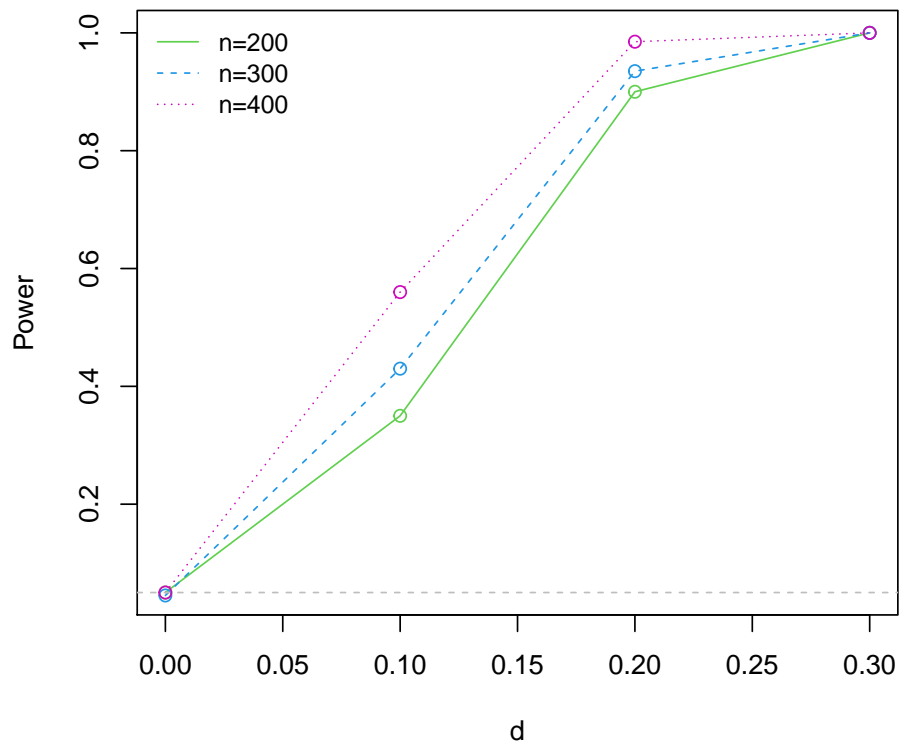


Figure S1: Displayed are the estimated power curves for simulation scenario A2. The parameter  $d$  controls the departure from the null and the power curves for  $n \in \{200, 300, 400\}$  are shown by solid, dashed and dotted lines. The dashed horizontal line at the bottom corresponds to the nominal level of  $\alpha = 0.05$ .

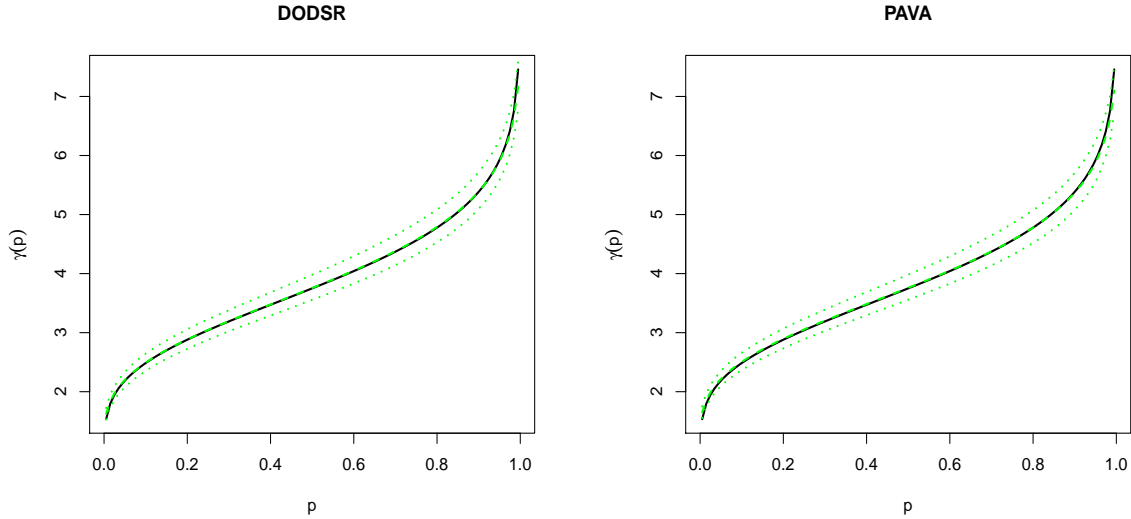


Figure S2: Displayed are estimates of additive effect  $\gamma(p) = \beta_0(p) + h(q_x(p))$  (solid) at  $q_x(p) = \frac{1}{n} \sum_{i=1}^n Q_{iX}(p)$  and its estimate  $\hat{\gamma}(p)$  averaged over 100 M.C. replications (dashed) along with point-wise 95% confidence interval (dotted) for scenario B,  $n = 400$ . Left: Estimates from the proposed DOSDR method. Right: Isotonic regression method with PAVA.

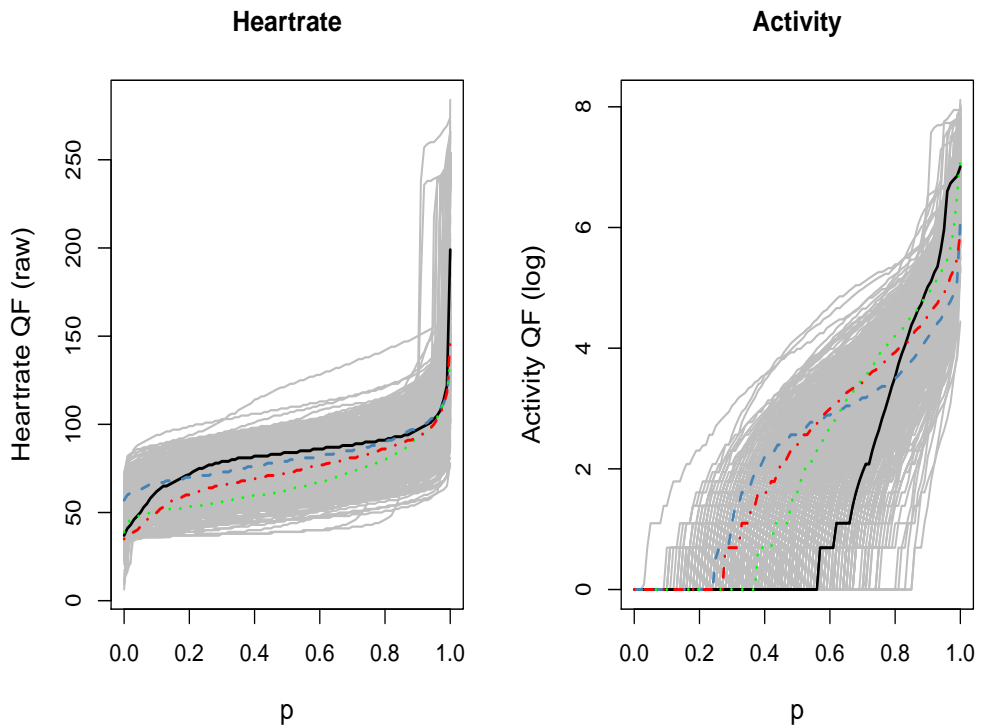


Figure S3: Subject-specific quantile functions of heart rate and log-transformed activity counts during 8 a.m.- 8 p.m. period. Color profiles show four randomly chosen participants.

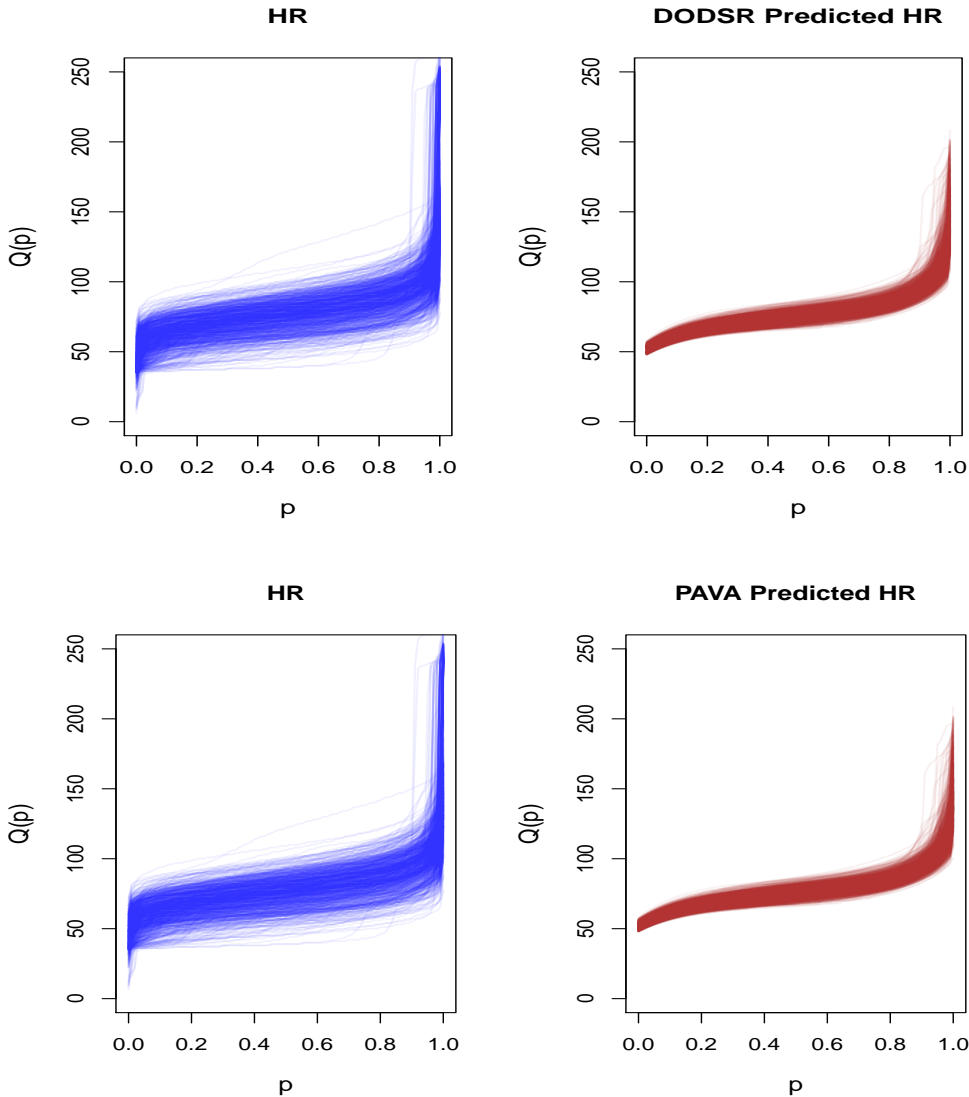


Figure S4: Top: LOOCV predictions of quantile functions of heart rate from DOSDR method based on age, sex, BMI and PA distribution. Bottom: LOOCV predictions of quantile functions of heart rate from PAVA method (Ghodrati and Panaretos, 2021) based on PA distribution.

## References

Ghodrati, L. and V. M. Panaretos (2021). Distribution-on-distribution regression via optimal transport maps. *arXiv preprint arXiv:2104.09418*.

Ghosal, R. and A. Maity (2022). A score based test for functional linear concurrent regression. *Econometrics and Statistics* 21, 114–130.

Huang, J. Z., C. O. Wu, and L. Zhou (2004). Polynomial spline estimation and inference for varying coefficient models with longitudinal data. *Statistica Sinica* 14, 763–788.

Yao, F., H.-G. Müller, and J.-L. Wang (2005). Functional linear regression analysis for longitudinal data. *The Annals of Statistics*, 2873–2903.